# ON THE INTERACTIONS BETWEEN CELLULOSE AND XYLAN, A BIOMIMETIC SIMULATION OF THE HARDWOOD CELL WALL

Sofia Dammström,[a] Lennart Salmén,[b*] and Paul Gatenholm[a]

The plant cell wall exhibits a hierarchical structure, in which the organization of the constituents on different levels strongly affects the mechanical properties and the performance of the material. In this work, the interactions between cellulose and xylan in a model system consisting of a bacterial cellulose/glucuronoxylan (extracted from aspen, *Populus tremula*) have been studied and compared to that of a delignified aspen fiber material. The properties of the materials were analyzed using Dynamical Mechanical Analysis (DMA) with moisture scans together with dynamic Infra Red -spectroscopy at dry and humid conditions. The results showed that strong interactions existed between the cellulose and the xylan in the aspen holocellulose. The same kinds of interactions were seen in a water-extracted bacterial cellulose/xylan composite, while unextracted material showed the presence of xylan not interacting with the cellulose. Based on these findings for the model system, it was suggested that there is in hardwood one fraction of xylan that is strongly associated with the cellulose, taking a similar role as glucomannan in softwood.

*Keywords: Bacterial cellulose; Biomimetic nanocomposites; Mechanical properties; Secondary cell wall;Xylan*

*Contact information: a: Biopolymer Technology, Department of Chemical and Biological Engineering, Chalmers University of Technology, Kemivägen 10, SE-412 96 Göteborg, Sweden; b: STFI-Packforsk AB, Box 5604, SE-114 86 Stockholm, Sweden; *Corresponding author: lennart.salmen@stfi.se*

## INTRODUCTION

The most common construction material present around us is the plant secondary cell wall, which we utilize in textiles and clothes, paper and hygiene products, wood, and timber, etc. The secondary plant cell wall exhibits a hierarchical structure, in which the organization of the constituents on different levels strongly affects the mechanical properties and the performance of the material. Despite the importance of this structural element in our every-day life, detailed information about the structural arrangement and the interfacial interactions between the cell wall constituents is still missing. Such knowledge would be of great importance for the development and design of future materials based on lignocellulosic components.

Already during the nineteen twenties and thirties, it was established that different layers of the wood cell wall had different compositions of what was denoted as lignin, cellulose, and other polysaccharides (Scarth et al. 1929; Ritter 1934; Gibbs 1935; Harlow 1939). A difficulty in separating lignin from the wall polysaccharides, especially from cellulose, was noted (Harlow 1939). In the early forties, Klauditz (1941) tried to extract pure fractions of each of the three main constituents (cellulose, lignin, and

hemicelluloses) but noticed that for example the cellulose fraction always contained some 3.5% hemicelluloses (pentosans). The interest in the different cell wall constituents grew during the fifties and sixties, and extensive efforts were made in the characterization of the components (Preston 1951; Asunamaa and Lange 1954; Balashov and Preston 1955; Sultze 1957; Liang and Marchessault 1959; Meier 1962). Timell (1967) stated that the number of wood species studied was so large that reliable generalizations about the abundance and properties of all major wood hemicelluloses could be made. Following the rising interest in the individual components, the knowledge of the organization and relations between hemicelluloses, cellulose, and lignin also increased. The multilayered description of the wood cell wall, as presented by Côté (1967), became universal. On a macroscopic level this description is still valid.

As the technical development has proceeded and more and more advanced analytical methods have become available, detailed information about interactions and organization of the cell wall constituents has been revealed. A number of reviews have been published (Terashima et al. 1993; Carpita and Gibeaut 1993; Carpita and McCann 2000), and sophisticated models of both the primary (McCann et al. 1992) and the secondary cell wall (Salmén and Olsson 1998; Ruel and Joseleau 2005; Lawoko et al. 2005) have emerged. A common standpoint in all models is that the cellulose fibrils are coated with hemicelluloses, forming larger units that are embedded in a lignin-hemicellulose matrix (Fengel and Wegener 1984). Furthermore, the hemicelluloses have been suggested to play an important role in the aggregation pattern of the cellulose by affecting the crystalline structure and changing the dimensions of the cellulose microfibril (Hackney et al. 1994; Uhlin et al. 1995; Iwata et al. 1998; Fujita and Harada 2001). It has also been suggested that the hemicelluloses affect the structure of lignin during the cell wall biosynthesis and that this structure may be altered by genetic modifications in the biosynthetic machinery of the hemicelluloses (Uhlin et al. 1995).

Ries and Vian (2004) published a study on the helicoidal pattern in the secondary cell walls and the possible role of glucuronoxylans in their construction. It was proposed that cellulose and glucuronoxylans are synchronically deposited prior to the lignification when the helicoids are built. The presence of a tight coating of cellulose microfibrils by the glucuronoxylans was indicated through surface labeling of cellulose, which revealed the existence of an acid coating bonded to the microfibrils. This hemicellulose coating of the microfibrils prevents the flocculation of the cellulose microfibrils (Dammström and Gatenholm 2006). The finding that glucuronoxylans possess surface charges and a molecular structure that regulate the fibrillogenesis and favor the formation of a cholesteric assembly gave rise to the proposition of a mechanism for the early construction of the secondary cell wall. In this mechanism, the carboxylic groups of the glucuronoxylan are arranged in a face-to-face manner, which generates electrostatic repelling forces that prevent the aggregation of the cellulose microfibrils and favor their parallel alignment. The structure then becomes consolidated by intercalation of lignin that interacts with the glucuronoxylan.

In order to further improve our understanding of the interactions between xylan and cellulose in hardwoods, a model system of bacterial cellulose and glucuronoxylan (extracted from Populus tremula) was investigated with DMA and dynamic FTIR and compared to the behavior of an aspen pulp. Prior to the measurements, the samples were

water extracted in order to remove loosely present xylans, with the purpose of probing the existence of any specific interactions between remaining xylans and cellulose in the samples. Here the use of dynamic FTIR provides for the ability to investigate such molecular interactions in composite materials (Noda et al. 1983; Åkerholm and Salmén 2001).

## MATERIALS AND METHODS

### Aspen Holocellulose

Match-sized sticks of aspen (*Populus tremula*) wood were dried in a vacuum oven at 50 $^{o}$C over night. Two batches were made simultaneously, each of them starting from 20 gram dry wood sticks, which were placed in two three-necked round-bottomed flasks. Each flask was charged with a mixture of 50 ml 1.33M sodium chlorite, 50 ml 1.66 M sodium acetate, and 2 ml concentrated acetic acid and diluted to a total of 400 ml with deionized water and heated to 70 $^{o}$C. The chlorite/acetate/acid- solution was added to each portion of the aspen wood-sticks, and the slurries were left under magnetic stirring at 70 $^{o}$C. After 30 minutes a second addition of 50 ml sodium chlorite and 2 ml acetic acid was made to each flask. Sodium chlorite and acetic acid were then added every 24 h during 6 days (Wise et al. 1946; Timell 1961). Nitrogen was flushed through the flasks for 5 hours to remove the remaining chlorine gas. Solids were filtered off using a Büchner funnel with a fine nylon mesh and washed with 5x1 liter deionized water (50 $^{o}$C). The holocellulose was dried in a vacuum oven at 50 $^{o}$C overnight resulting in a dry weight of 24.6 gram, ~62% of the initial dry wood. The relative composition of the holocellulose is given in Table 1. Fiber-oriented sheets of a grammage of 22 g/m$^2$, formed in a Formette Dynamique (French sheet former), were used for both the DMA- and the dynamic FTIR-measurements.

**Table 1.** The Relative Carbohydrate Composition of the Aspen Holocellulose and the O-acetyl-(4-O-methylglucurono)xylan; % of Total Anhydrosugars.

| Anhydrosugar | Water-extr. Composite rel. comp. % | Aspen holocellulose rel. comp. % |
|---|---|---|
| Glucose | 83.5 | 84 |
| Xylose | 15.9 | 12.9 |
| Galactose | n.d. | n.d. |
| Rhamnose | n.d. | 0.1 |
| Mannose | 0.6 | 3 |
| Glucosidic acid | <2 | <2 |
| n.d. non detectable | | |

### O-acetyl-(4-O-methylglucurono)xylan

The O-acetyl-(4-O-methylglucurono)xylan was obtained by DMSO-extraction of aspen holocellulose, prepared according to the procedure described above. Using a holocellulose:DMSO ratio 1:20, extraction was made for 24 h at room temperature, followed by additionally 24h at 60 $^{o}$C. The holocellulose/DMSO-slurry was filtered on a glass filter, and the filtrate was refiltered once. The extracted xylan was precipitated by pouring the filtrate into a mixture of 99% (v/v) ice-cold ethanol and 1% (v/v) acetic acid

($V_{ethanol}$ = 6x $V_{filtrate}$). After refrigeration over night, the xylan was filtered on a glass filter and washed with ~500 ml 99% ethanol. The O-acetyl-(4-O-methylglucurono)xylan was then dissolved in ~150 ml deionized water and freeze-dried. The resulting carbohydrate composition of the xylan is presented in Table 2. The xylan had $DS_{Acetyl}$ = 0.46 as determined by $^1$H-NMR and a molecular weight of ~12500, determined with size exclusion chromatography.

**Table 2.** Carbohydrate Composition of the O-acetyl-(4-O-methylglucurono)xylan.

| Anhydrosugar | Xylan, rel. comp. % |
|---|---|
| Xylose | 94 |
| Glucose | 3 |
| Mannose | 2.2 |
| Rhamnose | <1 |
| Galactose | <1 |

## Bacterial Cellulose/O-acetyl-(4-O-methylglucurono)xylan Nanocomposites

The cellulose was produced by static cultivation of Acetobacter Xylinum, sub specie BPR2001, in a fructose/CSL medium (Matsuoka et al. 1996) at 30 $^o$C. The bacteria were grown in 400 ml Erlenmeyer flasks containing 100 ml of media. The cultivation time varied between 2 to 3 weeks. The produced cellulose pellicles were heated in 1M NaOH at 80 $^o$C for 1h followed by repeated boiling in deionized water in order to remove the bacteria and to exchange remaining media. The washed cellulose was stored in diluted ethanol in a refrigerator (to prevent drying and to avoid contamination).

Nanocomposites with an original composition of 50% (w/w) bacterial cellulose and 50% (w/w) xylan were prepared according to the following procedure (Dammström et al. 2005). A microfibril-suspension of bacterial cellulose was obtained by homogenizing bacterial cellulose pellicles in a laboratory blender. The xylan was dissolved in water at 95 $^o$C for 15 minutes and centrifuged, which removed a few percent insoluble xylan. The microfibril suspension was then mixed with the xylan, and the suspension was allowed to interact for 30 minutes at room temperature before being poured into a polystyrene petri-dish and dried at 23 $^o$C, 50% relative humidity, RH.

## Water-extraction

A Soxhlet-device was used for water extraction of the aspen holocellulose and the nanocomposite. To avoid contamination with fibers and other substances, an extraction-thimble made from a fine metal mesh was used instead of an ordinary cellulose-based one. The mesh was washed in toluene, water and acetone prior to its use. Extraction was made using deionized water during 24h and the extraction water was collected and freeze-dried in order to recover the xylan. This procedure removed ca 85% of the xylan from the nanocomposite (Table 1) while the holocellulose was left practically unaffected.

## DMA

The DMA-equipment used was a Perkin-Elmer DMA7 operating in tension mode. A dynamic deformation was applied at a frequency of 1Hz. The static load was set to equal 120% of the dynamic load, keeping the amplitude constant at 3 μm. Measurements were performed in humidity scans from 30-90% RH after an initial conditioning at 30%

RH for 30 minutes. The scan rate used was 1% RH/min. Scanning at a lower speed did not affect the results. The humidity scan was created by a computer controlled humidifier which produces humid air by mixing dry and fully saturated air streams. The storage modulus, recalculated as relative storage modulus (set to 100% at 30% RH), and the phase loss angle were recorded.

### Dynamic FT-IR Spectroscopy

Spectra were recorded on an FTS 6000 FTIR spectrometer (Digilab Inc., Randolph, MA, USA) using a liquid nitrogen cooled MCT (Mercury Cadmium Telluride) detector. 15x25 mm sized samples were mounted in the holders of a stretching device (PM-100) placed in a Temperature Control System (TC-100) (MAT Inc., Troy, ID, USA). The spectra were recorded in step-scan mode at 30 $^{o}$C. The scanning speed was 0.5 Hz, and the phase modulation frequency was 400 Hz. A sinusoidal strain (<0.3%) with a frequency of 16 Hz was applied to the samples during the measurements. The IR radiation was polarized at either $0^{o}$ or $90^{o}$ relative the stretching direction of the sample. The obtained interferrograms were Fourier-transformed, and a triangular apodization function was applied. The resulting in-phase and out-of-phase spectra were divided by the static spectra and baseline corrected at 1780 $cm^{-1}$. After baseline correction the two signals were converted into a phase spectrum and a magnitude spectrum. The magnitude was normalized to 1 at 1435 $cm^{-1}$, and new in-phase and out-of phase spectra were calculated from the normalized magnitude. When recording the spectra at 85% RH, the TC-100 was connected to a humidity generator (VTI Corp., Hialeah, FL, USA).

## RESULTS AND DISCUSSION

Mechanical spectroscopic testing as dynamic mechanical analysis, DMA, and dynamic FTIR are methods suitable for revealing the common behavior of materials whereby with the use of component sensitive parameters, as humidity or temperature, one is able to identify the contribution to the overall behavior of individual components. In these studies the moisture sensitivity of the xylan component has been utilized.

### DMA

As can be seen in Fig. 1, the extracted composite and the aspen holocellulose showed very similar behavior with regard to the stiffness development with increasing humidity. The gradual decrease in modulus derives from a reduced number of hydrogen bonds joining polysaccharide moieties as a consequence of the increased surrounding relative humidity, an effect that may be seen in most biological materials. In a previous study (Dammström et al. 2005), the non-extracted cellulose/xylan composite showed a quite different behavior, having a pronounced softening decrease of the modulus, at about 85% surrounding relative humidity, very much in similarity with the behavior measured for a pure film of glucuronoxylan. The cellulose itself showed no such decrease in the modulus curve in this RH-range. Since there was as much as 50% O-acetyl-(4-O-methylglucurono)xylan in the non-extracted composite, it is reasonable to believe that in that case, the softening is caused by plasticization of the bulk xylan in a two-phase

system. In the water-extracted composite and the aspen holocellulose, the amount of xylan is lower, and a possible interaction between the remaining xylan and the cellulose may prevent any softening to be clearly visible. Due to this possible interaction with the cellulose, the softening of the water-extracted composite is spread over a wider interval as compared to the non-extracted composite.

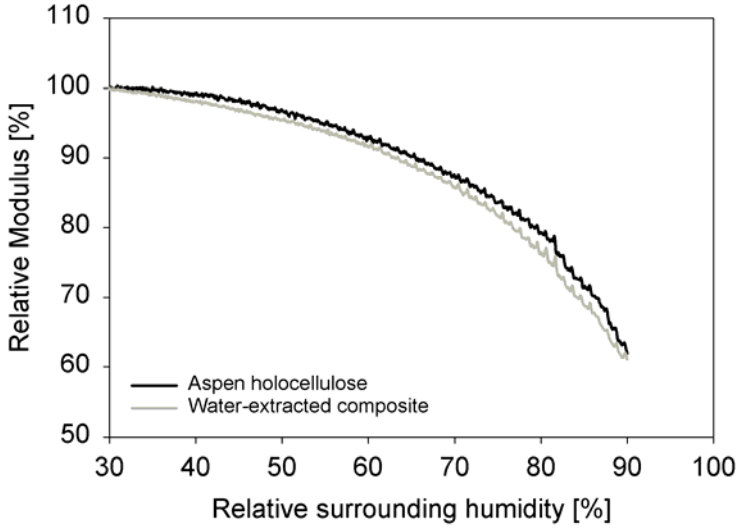


**Fig. 1.** Softening behavior of the aspen holocellulose and water-extracted nanocomposite as a function of surrounding relative humidity at 30 $^{o}$C.

## Dynamic FTIR

In dynamic FTIR-spectroscopy the spectrum is recorded while the sample is stretched by a sinusoidal strain. The stretching induces a change in direction or conformation of the dipole moment for those molecules that are affected by the load. Depending on the local surroundings, the molecules in the sample will respond in different ways, and either a positive, or a negative absorption band will occur. Groups that stay unaffected by the stretching and do not participate in the load transfer will not give rise to any absorption bands in the dynamic FTIR spectrum. Two different signals are recorded during the measurement, one in-phase- and one out-of-phase- signal. The in-phase signal corresponds to the direct, i.e. the elastic, component of the sample while the out-of-phase signal corresponds to the time-delayed, i.e. the viscous, component (Noda et al. 1983). Figure 2A shows the dynamic FTIR-spectra of the water-extracted composite recorded at 0% RH while Figure 2B shows that at 85% RH.

According to literature (Hinterstoisser et al. 2001), a signal from C-O-H bending in the cellulose molecule appears at 1435 $cm^{-1}$, which was also seen as a strong, nicely split signal in the spectrum. Another nicely split signal was visible at 1275 $cm^{-1}$, originating from $CH_2$-wagging in the cellulose molecule, (Liang and Marchessault 1959; Hinterstoisser et al. 2001) as also visible from the pure bacterial cellulose spectra in Figure 2C. In addition to the elastic signals, viscous signals were also present at 1435 $cm^{-1}$ and 1275 $cm^{-1}$, arising from secondary transitions of side groups. Two elastic signals could be assigned to the O-acetyl-(4-O-methylglucurono)xylan molecule. One broad peak

at ~1740 $cm^{-1}$ corresponded to the C=O bond in the acetyl group and in the glucuronic acid, and one peak at 1245 $cm^{-1}$ corresponded to the C-O-R link in the acetyl group (Marchessault 1962). The broadness of the 1740-peak probably originates from the fact that the two carbonyl bonds are not totally equal. The C=O bond of the acetyl group is shifted slightly different than the C=O bond in the glucuronic acid, thereby causing a broadening of the peak. Comparable measurements of glucuronoxylan showed that this polymer was plasticized by water and underwent a moisture-induced transition at about 80% RH (Dammström et al. 2005). One could therefore expect an increased viscous signal at xylan-specific wavenumbers (1740 $cm^{-1}$ and 1245 $cm^{-1}$) when recording the spectrum at 85% RH. As seen in Figure 2B, that was not the case. The presence of elastic signals from both the xylan and the cellulose, in combination with the absence of viscous xylan-signals at the higher humidity, suggests that there are interactions present between the two components that hinder the viscous behavior of the O-acetyl-(4-O-methylglucurono)xylan. Also in this case there was no major difference between the spectra recorded at dry and humid conditions although the overall viscous signal was somewhat increased.

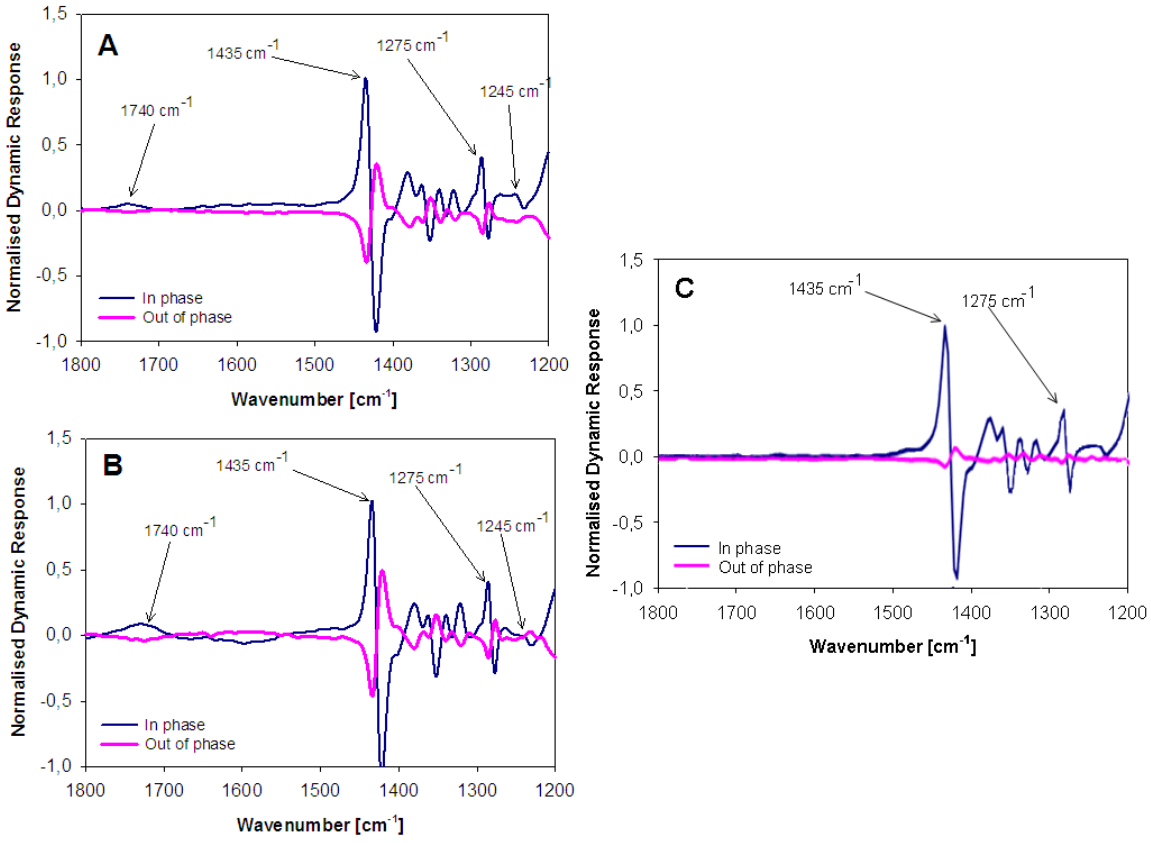


**Fig. 2.** Dynamic FTIR spectrum of water-extracted nanocomposite recorded at (A) 0% RH and (B) 85% RH, and for (C) bacterial cellulose recorded at 0% RH. T= 30 °C. In all cases the IR-irradiation used was of 0° polarization.

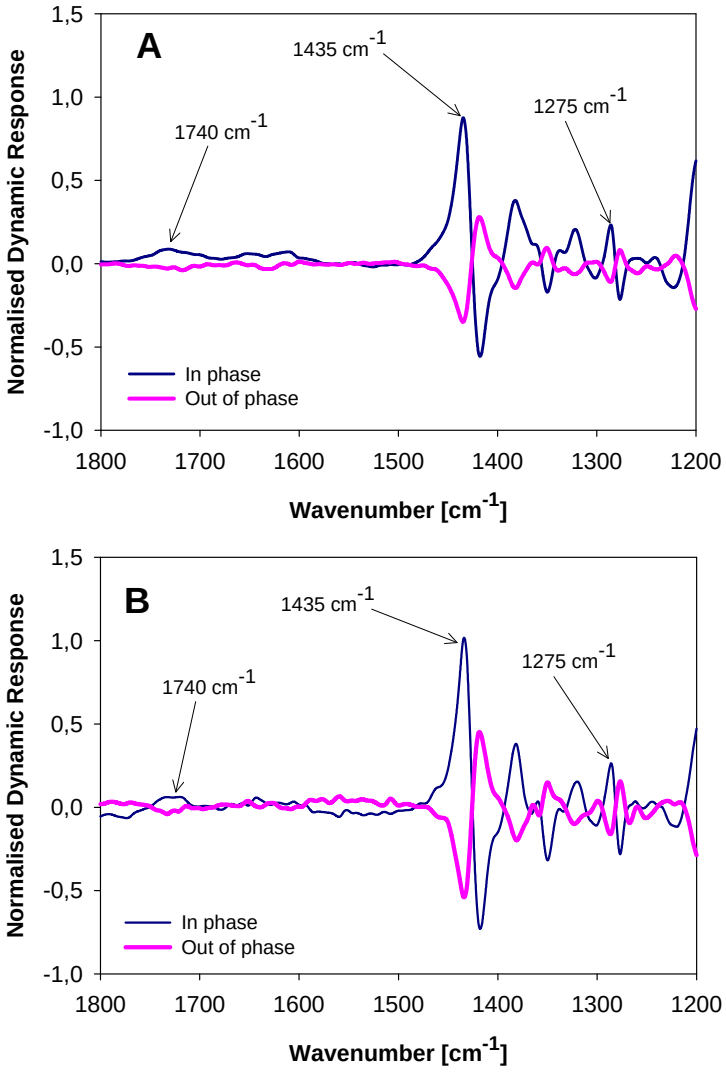


**Fig. 3.** Dynamic FTIR spectrum of oriented sheets of aspen holocellulose recorded at 0% RH, 30 °C, 0° polarization (A) and 85% RH, 30 °C, 0° polarization (B). The sinusoidal stretching was applied in the fiber direction.

The spectra from the aspen holocellulose sample, Fig. 3, looked very similar to those recorded for the water-extracted composite. Elastic and viscous signals from both the cellulose and the xylan appeared at about the same wavenumbers as for the extracted composite. Earlier studies performed on non-oriented sheets (Dammström et al. 2005) concluded that there are interactions between the cellulose and the xylan, and there was no reason to believe anything different for the oriented sheets studied here.

Measurements perpendicular to the fiber-orientation were also performed (Fig. 4). This spectrum showed very strong signals from the xylan at 1740 $cm^{-1}$ and also at 1245 $cm^{-1}$. For oriented paper sheets measurements perpendicular to the fiber direction reflect

to a larger extent the influence of connecting material between the fibers or the cellulose microfibrils (Åkerholm and Salmén 2002). Thus the larger response of groups associated to the xylan, also showing strong out-of phase signals in relation to the cellulose, should indicate a strong coupling between these components. This suggests that xylan acts as a connection between the cellulose microfibrils.

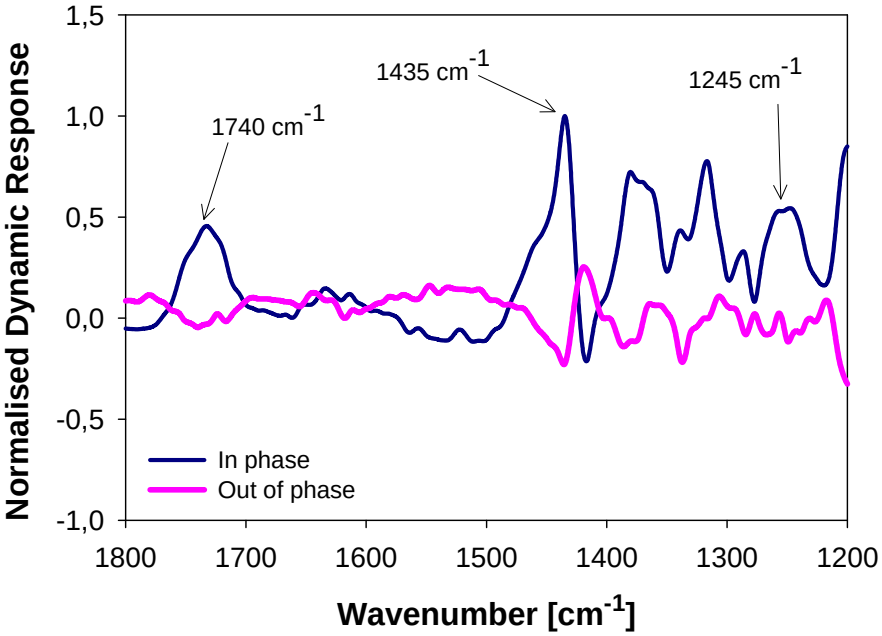


**Fig. 4.** Dynamic FTIR spectrum of oriented sheets of aspen holocellulose recorded at 0% RH, 30 $^{o}$C, 0$^{o}$ polarization. The sinusoidal stretching was applied transverse to the fiber direction.

## CONCLUSIONS

The results from the DMA- and the dynamic FTIR measurements suggested that there were strong interactions between the cellulose and the xylan in the aspen holocellulose. The same kind of interactions were seen in the water-extracted bacterial cellulose/O-acetyl-(4-O-methylglucurono)xylan composite. In its native state, aspen wood contains about 24% O-acetyl-(4-O-methyl-glucurono)xylan (Timell 1967), which to a large extent is lost during preparation of the holocellulose. One may speculate that the remaining ~13% indeed is strongly interacting with the cellulose and thereby unaffected by the delignification, while the rest of the xylan is associated to the lignin and thereby lost during this preparation process. In this respect the aspen wood is behaving in a similar way as the cellulose/xylan composite for which the water extractions that were carried out here also removed loosely present xylan, leaving only the strongly associated xylan left. This, in a similar way, changed the material characteristics form, being strongly affected by xylan (Dammström et al. 2005), to the one here studied, showing strong interactions between xylan and cellulose. Thus it could in fact be that there are two different fractions of xylan present in aspen wood, one fraction that is associated with the

cellulose and one fraction associated with the lignin. These findings are in line with the results obtained by use of labeling techniques, reported by Ruel et al. (2005), indicating a non-branched xylan preferably associated with the cellulose while a more branched type is preferably deposited together with the lignin. Thus the xylan that is more associated to the cellulose could be speculated to have a similar role as the glucomannan in softwood.

Based on the findings in this study, a schematic model of the secondary cell wall in non-coniferous wood is proposed (Fig. 5). In comparison, this model resembles the one proposed by Ries and Vian (2004), as described in detail in the introduction.

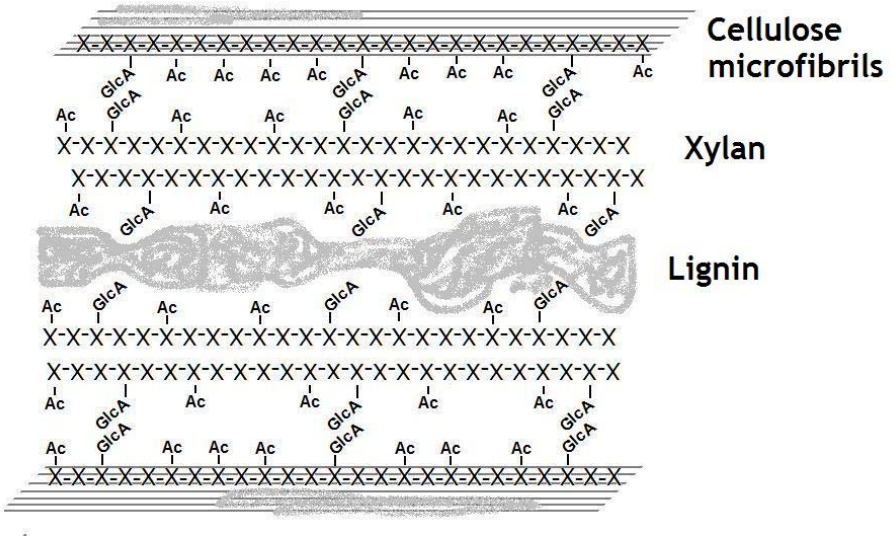


**Fig. 5.** Schematic picture of a proposed model for the arrangement of cellulose, xylan and lignin in the secondary cell walls of aspen wood. Note that the xylan has been greatly enlarged for better illustration. Gray areas represent lignin.

## ACKNOWLEDGMENTS

The Bo Rydin Foundation for Scientific Research is gratefully acknowledged for financial support. The authors wish to express their gratitude to Anne-Mari Olsson and Jasna Stevanic at STFI-Packforsk for help with the DMA and FTIR measurements. Anders Mårtensson is also acknowledged for carrying out the AFM-imaging.

## REFERENCES CITED

Åkerholm, M., and Salmén, L. (2001). "Interactions between wood 833 polymers studied by dynamic FT-IR spectroscopy." *Polymer* 834(42), 963-969.

Åkerholm, M., and Salmén, L. (2002). "Dynamic FTIR spectroscopy for carbohydrate analysis of wood pulps." *J. Pulp Pap. Sci.* 28(7), 245-249.

Asunamaa, S., and Lange, W. (1954). "The distribution of the components in the plant-cell wall. VII. The distribution of 'cellulose' and 'hemicellulose' in the cell wall of spruce, birch, and cotton," *Svensk Papperstidn.* 57, 501-516.

Balashov, V., and Preston, R. (1955). "The fine structure of cellulose and other microfibrillar substances," *Nature* 176, 64-65.

Carpita, N. C., and Gibeaut, D. M. (1993). "Structural models of primary cell walls in flowering plants: Consistency of molecular structure with the physical properties of the walls during growth," *Plant Journal* 3(1), 1-30.

Carpita, N., and McCann, M. (2000). "The cell wall," in *Biochemistry & Molecular Biology of Plants*, B. Buchanan, W. Gruissem, and R. Jones (eds.) American Society of Plant Physiologists, Rockville MD, 52-108.

Côté, W. (1967). *Wood Ultrastructure*, University of Washington Press, Seattle WA.

Dammström, S., and Gatenholm, P. (2006). "Preparation and properties of cellulose/ xylan nanocomposites," in *Characterization of the Cellulosic Cell Wall*, Proceedings of a Workshop, Grand Lake, CO, United States, Aug. 25-27, 2003; D. Stokke and L. Groom (eds) Blackwell Publishing, Ames, Iowa, 53-63.

Dammström, S., Salmén, L., and Gatenholm, P. (2005). "The effect of moisture on the dynamical mechanical properties of bacterial cellulose/glucuronoxylan nanocomposites," *Polymer* 46(23), 10364-10371.

Fengel, D., and Wegener, G. (1984). *Wood: Chemistry, Ultrastructure, Reactions*, de Gruyter, Berlin

Fujita, M., and Harada, H. (2001). "Ultrastructure and formation of wood cell wall," in *Wood and Cellulosic Chemistry (2nd edition)*, D, Hon and N. Shiraishi (eds.) Marcel Dekker, New York, NY, 1-49

Gibbs, R. (1935) "Studies of wood I. The cell wall," *Canadian Journal of Research* 12, 715-726.

Hackney, J., Atalla, R., and VanderHart, D. (1994). "Modification of crystallinity and crystalline structure of Acetobacter xylinum cellulose in the presence of water-soluble β -1,4-linked polysaccharides: 13C-NMR evidence," *Int. J. Biological Macromolecules* 16(4), 215-218.

Harlow, W. (1939). "Chemistry of the plant cell wall. IX. Further studies on the isolation of lignin, cellulose and other components in woody cell walls," *Paper Trade Journal* 109(18), 38-42

Hinterstoisser, B., Åkerholm, M., and Salmén, L. (2001). "Effect of fiber orientation in dynamic FTIR study on native cellulose," *Carbohydrate Research* 334(1), 27-37.

Iwata, T., Indrarti, L., and Azuma, J-I. (1998). "Affinity of hemicellulose for cellulose produced by *Acetobacter xylinum*," *Cellulose* 5(3), 215-228.

Klauditz, W. (1941). "The cellulose in the cell walls of hardwoods," *Papierfabrikant* 39, 225-228.

Lawoko, M., Henriksson, G., and Gellerstedt, G. (2005). "Structural differences between the lignin-carbohydrate complexes present in wood and in chemical pulps," *Biomacromolecules* 6(6), 3467-3473.

Liang, C., and Marchessault, R. (1959). "Infrared spectra of crystalline polysaccharides II. Native celluloses in the region from 640-1700 $cm^{-1}$," *J. Polymer Science* 39, 269-278.

Marchessault, R. (1962). "Application of infrared spectroscopy to cellulose and wood polysaccharides," *Pure and Applied Chemistry* 5, 107-129.

Matsuoka, M., Tsuchida, T., Matsushita, K., Adachi, O., and Yoshinaga, F. (1996). "A synthetic medium for bacterial cellulose production by *Acetobacter xylinum* subsp. *Sucrofermentans*," *Bioscience, Biotechnology, Biochemistry* 60(4), 575-579.

McCann, M. C., Wells, B., and Roberts, K. (1992). "Complexity in the spatial localization and length distribution of plant cell-wall matrix polysaccharides," *J. Microscopy* 166(1), 123-136.

Meier, H. (1962). "Chemical and morphological aspects of the fine structure of wood," *Pure and Applied Chemistry* 5, 37-52.

Noda, I., Dowery, A. E., and Marcott, C. (1983). "Dynamic infrared linear dichroism of polymer films under oscillatory deformation." *Polymer Science: Polymer Letters Editio,* 21, 99-103.

Preston, R. (1951). "Biophysical aspects of polysaccharide structure in plants," *Progress in Biophysics* 2, 17-50.

Reis, D., and Vian, B. (2004). "Helicoidal pattern in secondary cell walls and possible role of xylans in their construction," *Comptes Rendus Biologies* 327, 785-790.

Ritter, G. (1934). "Structure of the cell wall of wood fibers," *Paper Ind.* 16, 178-183.

Ruel, K. and Joseleau, J-P. (2005). "Deposition of hemicelluloses and lignins during secondary wood cell wall assembly," in *The Hemicelluloses Workshop 2005,* K. M. Entwistle and J. C. F. Walker (eds.) Wood Techn. Res. Centre, Christchurch, 103-113.

Salmén, L., and Olsson, A-M. (1998). "Interaction between hemicelluloses, lignin and cellulose: Structure-property relationships," *J. Pulp Pap. Sci.* 24(3), 99-103.

Scarth, G., Gibbs, R., and Spier, J. (1929). "Studies of the cell walls in wood. I. The structure of the cell wall and the local distribution of the chemical constituents," *Proceedings and Transactions of the Royal Society of Canada* 23(V), 269-279.

Sultze, R. (1957). "The developing tissues of aspenwood," *Tappi* 40, 984-994.

Terashima, N., Fukushima. K., He, L.-F., and Takabe, K. (1993). "Comprehensive model of the lignified plant cell wall," in *Forage Cell Wall Structure and Digestibility,* H. G. Jung, D. R. Buxton, R. D. Hatfield, and J. Ralph (eds.), Madison, WI, ASA-CSSA-SSSA, 247-270.

Timell, T. (1961). "Isolation of galactoglucomannans from the wood of gymnosperms," *Tappi* 44, 88-96.

Timell, T. (1967). "Recent progress in the chemistry of wood hemicelluloses," *Wood Sci. Technol.* 1(1), 45-70.

Uhlin, K., Atalla, R., and Thompson, N. (1995). "Influence of hemicelluloses on the aggregation patterns of bacterial cellulose," *Cellulose* 2(2), 129-144.

Wise, L., Murphy, M., and D'Addieco, A. (1946). "Chlorite holocellulose, its fractionation and bearing on summative wood analysis and on studies on the hemicelluloses," *Paper Trade J.* 122(2), 35-43.

Article submitted: July 2, 2008; Peer-review completed: Oct. 4, 2008; Revised version received and accepted: Nov. 3, 2008; Published: Nov. 5, 2008.